Characterization of Depressive States in Bipolar Patients Using Wearable Textile Technology and Instantaneous Heart Rate Variability Assessment

Gaetano Valenza, *Member, IEEE*, Luca Citi, *Member, IEEE*, Claudio Gentili, Antonio Lanatá, *Member, IEEE*, Enzo Pasquale Scilingo, *Member, IEEE*, and Riccardo Barbieri, *Senior Member, IEEE*

***Abstract*—The analysis of cognitive and autonomic responses to emotionally relevant stimuli could provide a viable solution for the automatic recognition of different mood states, both in normal and pathological conditions. In this study, we present a methodological application describing a novel system based on wearable textile technology and instantaneous nonlinear heart rate variability assessment, able to characterize the autonomic status of bipolar patients by considering only electrocardiogram recordings. As a proof of this concept, our study presents results obtained from eight bipolar patients during their normal daily activities and being elicited according to a specific emotional protocol through the presentation of emotionally relevant pictures. Linear and nonlinear features were computed using a novel point-process-based nonlinear autoregressive integrative model and compared with traditional algorithmic methods. The estimated indices were used as the input of a multilayer perceptron to discriminate the depressive from the euthymic status. Results show that our system achieves much higher accuracy than the traditional techniques. Moreover, the inclusion of instantaneous higher order spectra features significantly improves the accuracy in successfully recognizing depression from euthymia.**

***Index Terms*—Bipolar disorder, bispectrum, heart rate variability (HRV), high-order statistics, mood recognition, nonlinear analysis, point process, wearable systems, wearable textile monitoring, Wiener–Volterra model.**

Manuscript received August 20, 2013; revised January 10, 2014; accepted February 19, 2014. Date of publication February 21, 2014; date of current version December 30, 2014. This work was supported in part by EU Commission under Contract ICT-247777 Psyche and by the Department of Anesthesia, Critical Care & Pain Medicine, Massachusetts General Hospital, and Harvard Medical School, Boston, MA, USA.

G. Valenza is with the Research Center E. Piaggio and also with the Department of Information Engineering, University of Pisa, Pisa, Italy, and also with the Neuroscience Statistics Research Laboratory, Harvard Medical School, Massachusetts General Hospital, Boston, MA, 02114 USA, and also with the Massachusetts Institute of Technology, Cambridge, MA 02139 USA (e-mail: g.valenza@ieee.org).

L. Citi is with the Neuroscience Statistics Research Laboratory, Harvard Medical School, Massachusetts General Hospital, Boston, MA 02114 USA, and also with the Massachusetts Institute of Technology, Cambridge, MA 02139 USA and also with the School of Computer Science and Electronic Engineering, University of Essex, Colchester, CO4 3SQ, U.K. (e-mail: lciti@neurostat.mit.edu).

C. Gentili is with the Department of Surgical, Medical, Molecular, and Critical Area Pathology, Section of Psychology, University of Pisa, 56100 Pisa, Italy (e-mail: claudio.gentili@med.unipi.it).

A. Lanatá and E. P. Scilingo are with the Research Center E. Piaggio and also with the Department of Information Engineering, University of Pisa, 56100 Pisa, Italy (e-mail: a.lanata@centropiaggio.unipi.it; e.scilingo@centropiaggio.unipi.it).

R. Barbieri is with the Neuroscience Statistics Research Laboratory, Harvard Medical School, Massachusetts General Hospital, Boston, MA 02114 USA, and also with the Massachusetts Institute of Technology, Cambridge, MA 02139 USA (e-mail: barbieri@neurostat.mit.edu).

Color versions of one or more of the figures in this paper are available online at http://ieeexplore.ieee.org.

Digital Object Identifier 10.1109/JBHI.2014.2307584

I. Introduction

A. Bipolar Disorder

Bipolar disorder is one of the most diffuse psychiatric disorders in the western world. It has been demonstrated that more than two million Americans have been diagnosed with such a mood alteration [1] and, in 2005, about 27% of the adult European population, from 18 to 65 years of age, is or has been affected by at least one mental disorder [2]. In general, bipolar patients can experience different types of mood alterations, generally defined as *episodes*, typically limited over defined time intervals and subjected to spontaneous remissions or relapses. Four possible episodes are generally described: depression, mania, hypomania, (a less severe form of mania) and mixed state. When the subject undergoes a remission phase, clinicians refer to his condition as *euthymia*.

During depressive episodes, sadness and desperation are often the most prominent symptoms, although different other complain are present, including cognitive complaints, suicidal thoughts, or somatic symptoms like gastrointestinal pain, sexual, and urogenital disorders. Neurovegetative symptoms such as loss of appetite and insomnia may be present as well. Patients might also experience pathological ideas of self-pity and guilt, which might grow toward delusional states. During mania (and hypomania), a pathologically increased physical and mental activity causes loss of attention, reduction of the necessity to sleep, and an increased speed of the stream of thoughts that eventually leads to incoherence. Thus, the subject is often hyperactive but often without specific purposes. Moreover, (hypo)mania is often dominated by a feeling of an excited mood with the idea of grandiosity and hypertrophic self-esteem. In mania (but not in hypomania), such feelings might become delusional with a progressive detachment from the objective evaluation of the external world. Mixed state is characterized by the contemporary presence of depressive and maniac or hypomaniac symptoms (e.g., patients can have delusions of grandiosity but also have thoughts of guilt, can have motor retardation but increased speed of their thoughts). Generally, a diagnosis of the mixed state is made if the patient fulfills at the same time the criteria for (hypo)maniac and for depressive episode. In between these episodes, patients typically experience periods of relatively good affective balance (euthymia). Although remissions

happen in the natural history of bipolar disorders, this condition is often fostered by treatments (both pharmacological and nonpharmacological).

Bipolar disorder is a chronic disease: Even if a period of remission could occur, bipolar patients manifest episodes of mood alteration for decades. Despite its prevalence and high cost of treatment [1], this disease may go undetected for years before diagnosed and treated. Patients with mood disorders might experience a heterogeneous pattern of symptoms which might be present even during euthymic periods as subthreshold mood alterations. Moreover, the phenomenology and severity of the symptoms, the number and duration of the episodes, as well as the time interval between them are often not consistent among subjects. Another open issue in diagnosing bipolar disorders as well as the great majority of mental disorders is that symptoms are assessed by rating scales both administered by clinicians and self-completed by patients. So far, neither biological markers nor physiological correlates were found to be specific and sensitive enough to be used for clinical purposes [3], [4]. In this preliminary study, five patients were monitored over a period of up to 90 days and experienced only depressive and euthymic episodes. Our goal, therefore, at least within this early acquisition phase, is to discriminate depression from euthymia. In the next section, we will describe a novel system able to robustly distinguish depressive from euthymic episodes in bipolar patients by using wearable textile technology and taking inspiration from the mathematical theory of the nonlinear (NL) dynamical system.

B. Analysis of Cardiovascular Dynamics in Bipolarism

Previous studies on bipolar disorders highlighted changes in several physiological systems including sleep (as evaluated both with EEG and behaviorally) [5]–[7], circadian heart rate rhythms [8], [9], cortisol dynamics [10]–[12], as well as the autonomic nervous system (ANS) functionality [13], [14]. One important criterion for the inclusion of bipolar patients in studies involving ANS monitoring is their full compliance with the required recording procedures. There are also sensitive issues in trying to avoid any possible stigmatization due to participation. For these reasons, wearable, comfortable, and unobtrusive systems, e.g., sensorized t-shirts [15]–[22] or gloves [23], [24], are strongly recommended.

Mood has been defined as a long-lasting, diffuse affective state that is not associated with a specific trigger [25]. In turn, emotions are considered transient, acute, and arousing responses to specific stimuli. It is well known, however, that mood status affects the normal emotional response, and for this reason, a possible assessment approach is to study the physiological variations provoked by external affective cues (e.g., [26]–[33]). Specifically, paradigms based on emotional reactions have been proven to be widely able to differentiate among different mood states both in normal [34] and pathological conditions [35], [36]. Therefore, in this study, we focus on the ANS changes induced by emotion-related tasks in bipolar patients. According to the previous psychophysiological considerations, it is reasonable to represent the cardiovascular system as a NL dynamical system and study it by means of "perturbation" analysis, meaning that the analysis will take into account observations during initial stable conditions (i.e., during rest) and after fast perturbations (i.e., emotional elicitation). Hypothesizing that the ANS responds with different time-varying heartbeat dynamics according to the patient's mood state, computational tools able to discern rapid dynamic changes with high-time resolution are the best candidates for providing optimal assessments. For this purpose, standard heart rate variability (HRV) analysis is not recommended, since it would require relatively long-time intervals of electrocardiogram (ECG) acquisitions [37], [38] and would be unable to detect instantaneous variations. To overcome these limitations, we propose a novel stochastic model of heartbeat dynamics based on point-process theory that is able to instantaneously assess the patient's mood state. To our knowledge, this approach provides a novel paradigm in the literature of psychiatric disorders. The core of the model is the definition of the interbeat probability function to predict the waiting time of the next heartbeat, i.e., the R-wave event, given a linear (L) and NL combination of the previous events.

The use of the point process theory allows for a fully parametric structure analytically defined at each moment in time, thus allowing to estimate instantaneous measures [27], [39]–[45] without using any interpolation method. It has been demonstrated that the inverse-Gaussian (IG) distribution well characterizes the interbeat probability function [39] and, in particular, a L [39] and NL [27], [42], [43], [45] combination of the past events has been previously taken into account. These methods have been demonstrated to provide a faster and more accurate time-varying assessment than other sliding window beat-to-beat-based methods [40]. In this study, we propose an improvement of the model by defining a NL combination of the derivative series of past events. The resulting quadratic nonlinear autoregressive integrative (NARI) model improves the achievement of stationarity [46] and consequently improves system identification. This powerful approach further considers an equivalent third-order input–output Wiener–Volterra model, allowing for the instantaneous estimation of the high-order polyspectra [47], such as bispectrum and trispectrum [48]. Along with mathematical and modeling reasons, such a NL model is also physiologically justified. Cardiovascular control mainly refers to the signaling of the sympathetic and parasympathetic nerves controlling the pacemaker cells in a NL way [49].

In this study, we validate the engagement of the NL terms of the model by performing a comparative analysis demonstrating how the inclusion of instantaneous higher order spectra (HOS) features indeed improves the accuracy and reduces the uncertainty (variance) in recognizing ANS depressive patterns. We further compare results from standard analysis with those obtained using the novel model proposed here. Data were collected within the European funded project PSYCHE whose goal is to discover possible correlations between the patterns of physiological/behavioral signs and mood fluctuations over short- and long-term monitoring (see details in Section II-A). This project proposes a novel approach for bipolar disease management based on the paradigm that a quasi-continuous monitoring in a natural environment provides parameters, indices, and trends

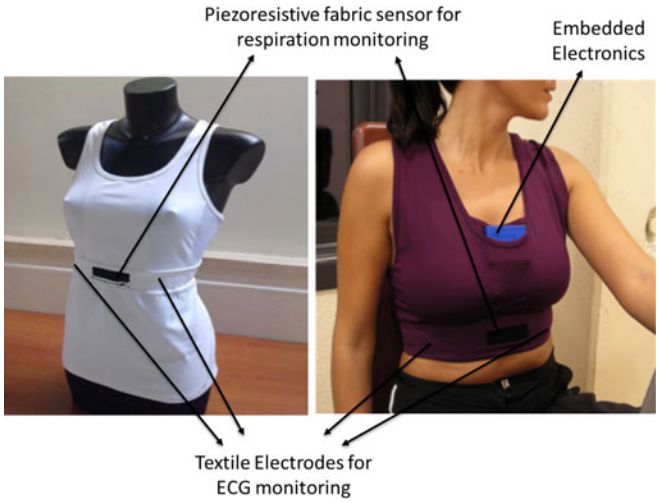

Fig. 1. Prototype of the PSYCHE wearable platform.

that will be used to assess mood status, support patients, predict and anticipate treatment response in its early phase, prevent relapse, and to alert physicians in case of a critical event.

II. Materials and Methods

A. PSYCHE Project and the Wearable Monitoring Platform

Data used in this study were collected within the European project PSYCHE (Personaliz ed monitoring SYstems for Care in mental HEalth), which is funded in the Seventh Framework Programme (FP7). The PSYCHE system [15]–[18] comprised a personal, pervasive, cost-effective, and multiparametric monitoring system based on textile electrodes and portable sensing devices for the long-term and short-term acquisition of data from an homogeneous class of patients affected by mood disorders. Currently, several physiological signals as well as behavioral parameters are taken into account as part of the PSYCHE project (e.g., ANS-related signs, voice, activity index, sleep pattern alteration, electrodermal response, biochemical markers). The core sensing system of the project, the PSYCHE platform developed by Smartex S.r.l., consists of a comfortable textile-based sensorized t-shirt that is embedded with fabric-based electrodes and acquires ECG, respiration signals, and body activity (accelerometers). Fig. 1 shows the wearable system prototype that employs textile electrodes to detect the ECG and piezoresistive sensors to acquire the respiration signal. In addition, a three-axial accelerometer embedded into the system tracks the movement. The PSYCHE platform is able to continuously acquire physiological data, stored in a Micro SD card for up to 24 h, using a lithium battery. The ECG is acquired by using a single lead configuration, 250 Hz of sampling rate and 16 bits of analog-to-digital conversion resolution. A user-friendly device such as a smartphone for monitoring environmental information such as light, temperature, and noise completes the PSYCHE platform.

Another novelty of the PSYCHE platform is the number of features estimated by a wide range of signal processing techniques, as opposed to previous studies carried out on this topic [5]–[9] where only a few parameters were included. Extracted from L and NL methods, these features will be investigated for finding possible relationships between physiological signs and mental disorders. This approach increases the sensitivity and the specificity of the system functionality and, as a consequence, the success rate. In this study, we focus on novel L and NL features of heartbeat dynamics which are crucial for the assessment of the depressive status in bipolar disorder. The reliability of the PSYCHE wearable platform, evaluated through the analysis of data gathered from the sensorized t-shirt, has been verified in our previous studies [16]–[19]. However, it is worthwhile mentioning that more than 90% of HRV and respiration activity signals recorded during long-term monitoring (about 18 h) were artifact free [17]. Such a high reliability is achieved through specific manufacturing choices. In particular, the use of dry textile-based electrodes provides comfort and reduces the rate of evaporation reaching electrochemical equilibrium between the skin and electrodes after a couple of minutes. Therefore, the signal quality is remarkably improved and kept as constant as possible. If the contact with the skin is not good due to size, the quality of the signals cannot be adequate for obtaining meaningful values. To avoid this problem, a preliminary check on the quality of the data is done using available shirts with different sizes before giving the system to the patients. The shirt was designed for females and males and was made of elastic fibers that allow for tight adhesion to the user's body, piezoresistive fibers to monitor fabric stretching (and consequently respiration activity), and metallic fibers knitted to create fabric electrodes to monitor the ECG.

B. Autoregressive Integrative Identification System

Instantaneous NL heartbeat dynamics can be predicted taking inspiration from the NL system identification theory, and in our case through the following NARI form:

$$E[y(k)] = y(k-1) + \gamma_0 \; + \sum_{i=1}^{M} \gamma_1(i)\,\Delta y(k-i) + \sum_{n=2}^{\infty} \sum_{i_1=1}^{M} \cdots \sum_{i_n=1}^{M} \gamma_n(i_1,\ldots,i_n) \prod_{j=1}^{n} \Delta y(k-i_j) \tag{1}$$

where $\Delta y(k-i) = y(k-i) - y(k-i-1)$ and $\Delta y(k-j) = y(k-j) - y(k-j-1)$, n is the degree of nonlinearity and M is the order, i.e., the number of past samples taken by each term. The autoregressive structure of (1) allows for the system identification with only exact knowledge of the output data and with only few assumptions about the input data. Here, we represent the NL physiological system by using NL kernels up to the second order, i.e., γ_0, $\gamma_1(i)$, and $\gamma_2(i,j)$. This choice of a second-order NARI system retains an important part of the nonlinearity of the system. In order to complete the NL system identification, it is necessary to link the NARI model to a general input–output form. By defining the extended kernels

$\gamma_1'(i)$ and $\gamma_2'(i,j)$ as

$$\gamma_1'(i) = \begin{cases} 1, & \text{if } i = 0 \\ -\gamma_1(i), & \text{if } 1 \le i \le M \end{cases} \tag{2}$$

$$\gamma_2'(i,j) = \begin{cases} 0, & \text{if } ij = 0 \wedge i + j \le M \\ -\gamma_2(i,j), & \text{if } 1 \le i \le M \wedge 1 \le j \le M \end{cases} \tag{3}$$

it is possible to map a quadratic NARI model to an *n*th-order input–output model [47]. After the input–output transformation of the kernels, the choice of a second-order autoregressive model allows evaluating all the high-order statistics (HOS) of the system, such as the dynamic bispectrum and trispectrum [50], [51]. In the following sections, we report the definition of the point-process framework of the heartbeat dynamics, as well as mathematical details on the derivation of the NL kernels and of the HOS tools.

C. NARI-Based Point-Process Models

To mathematically explain the point process framework, the following definitions are needed:

1) $t \in (0, T]$: the observation interval.
2) $0 \le u_1 < \cdots < u_k < u_{k+1} < \cdots < u_K \le T$: the times of the R-wave events.
3) $N(t) = \max\{k : u_k \le t\}$: the sample path of the $\{u_j\}_{j=1}^{J}$ counting process.
4) $dN(t)$: differential of $N(t)$. $dN(t) = 1$ in case of heartbeat event, $dN(t) = 0$ otherwise.
5) $\widetilde{N}(t) = \lim_{\tau \to t^-} N(\tau) = \max\{k : u_k < t\}$: left continuous sample path of $N(t)$.
6) $\mathrm{RR}_j = u_j - u_{j-1} > 0$: the jth R-R interval.

Given such definitions, and assuming that $\mathrm{RR}_j = f(\mathrm{RR}_{j-1}, \mathrm{RR}_{j-2}, \ldots, \mathrm{RR}_{j-n})$ (history dependence), the probability distribution of the waiting time $t - u_j$ until the next R-wave event follows an IG model [39]:

$$f(t|\mathcal{H}_t, \xi(t)) = \left[\frac{\xi_0(t)}{2\pi(t-u_j)^3}\right]^{\frac{1}{2}} \times \exp\left\{-\frac{1}{2}\frac{\xi_0(t)[t - u_j - \mu_{\mathrm{RR}}(t, \mathcal{H}_t, \xi(t))]^2}{\mu_{\mathrm{RR}}(t, \mathcal{H}_t, \xi(t))^2 (t - u_j)}\right\} \tag{4}$$

with $j = \widetilde{N}(t)$ as the index of the previous R-wave event before time t, $\mathcal{H}_t = (u_j, \mathrm{RR}_j, \mathrm{RR}_{j-1}, \ldots, \mathrm{RR}_{j-M+1})$, $\xi(t)$ the vector of the time-varing parameters, $\mu_{\mathrm{RR}}(t, \mathcal{H}_t, \xi(t))$ the first-moment statistic (mean) of the distribution, and $\xi_0(t) > 0$ the shape parameter of the IG distribution. Since $f(t|\mathcal{H}_t, \xi(t))$ indicates the probability of having a beat at time t given that a previous beat has occurred at u_j, $\mu_{\mathrm{RR}}(t, \mathcal{H}_t, \xi(t))$ can be interpreted as the most probable moment when the next beat could occur. The use of an IG distribution $f(t|\mathcal{H}_t, \xi(t))$, characterized at each moment in time, is motivated both physiologically (the integrate-and-fire initiating the cardiac contraction [39]) and by goodness-of-fit comparisons [41]. In previous works [40], [41], the instantaneous mean $\mu_{\mathrm{RR}}(t, \mathcal{H}_t, \xi(t))$ was expressed as a L combination of present and past R-R intervals (in terms of an AR model) and as a quadratic NL coupling of the heartbeat dynamics, based on a NL Volterra–Wiener expansion [42]. Here, we propose the novel NARI formulation based on (1) that allows us to define the instantaneous R-R mean as

$$\begin{aligned} \mu_{\mathrm{RR}}(t, \mathcal{H}_t, \xi(t)) &= \mathrm{RR}_{\widetilde{N}(t)} + \gamma_0 + \sum_{i=1}^{p} \gamma_1(i,t)\left(\mathrm{RR}_{\widetilde{N}(t)-i} - \mathrm{RR}_{\widetilde{N}(t)-i-1}\right) \\ &\quad + \sum_{i=1}^{q}\sum_{j=1}^{q} \gamma_2(i,j,t)\left(\mathrm{RR}_{\widetilde{N}(t)-i} - \mathrm{RR}_{\widetilde{N}(t)-i-1}\right) \\ &\quad \times \left(\mathrm{RR}_{\widetilde{N}(t)-j} - \mathrm{RR}_{\widetilde{N}(t)-j-1}\right) \end{aligned} \tag{5}$$

considering that the derivative R-R interval series improves the achievement of stationarity within the moving time window W (in this study, we have chosen $W = 70$ s) [46], [52]. Since $\mu_{\mathrm{RR}}(t, \mathcal{H}_t, \xi(t))$ is defined in continuous time, we can obtain an instantaneous R-R mean estimate at a very fine timescale (with an arbitrarily small bin size Δ), which requires no interpolation between heartbeat arrival times. Given the proposed parametric model, the NL indices of HRV will be defined as a time-varying function of the parameters $\xi(t) = [\xi_0(t), g_0(t), g_1(0,t), \ldots, g_1(p,t), g_2(0,0,t), \ldots, g_2(i,j,t)]$. The unknown time-varying parameter vector $\boldsymbol{\xi}(t)$ is estimated by means of a local maximum likelihood method [39], [53]. Briefly, given a local observation interval $(t - l, t]$ of duration l, we consider a subset $U_{m:n}$ of the R-wave events, where $m = N(t - l) + 1$ and $n = N(t)$ and, at each time t, we find the unknown time-varying parameter vector $\boldsymbol{\xi}(t)$ that maximizes the following local log-likelihood:

$$\begin{aligned} L(\boldsymbol{\xi}(t) \,|\, U_{m:n}) = &\sum_{k=m+P-1}^{n-1} w(t - u_{k+1}) \\ &\times \log[f(u_{k+1} \,|\, \mathcal{H}_{u_{k+1}}, \xi(t))] \\ &+ \log \int_{t-u_n}^{\infty} f(\tau \,|\, \mathcal{H}_{u_n}, \xi(t)) d\tau \end{aligned} \tag{6}$$

where $w(\tau) = e^{\varpi \tau}$ is an exponential weighting function for the local likelihood. We use a Newton–Raphson procedure to maximize the local log-likelihood in (6) and compute the local maximum-likelihood estimate of $\boldsymbol{\xi}(t)$ [53]. Because there is significant overlap between adjacent local likelihood intervals, we start the Newton–Raphson procedure at t with the previous local maximum-likelihood estimate at time $t - \Delta$, where Δ defines the time interval shift to compute the next parameter update. The model goodness-of-fit is based on the Kolmogorov–Smirnov (KS) test and associated KS statistics (see details in [39]). Moreover, autocorrelation plots are considered to test the independence of the model-transformed intervals [39]. Once the order $\{p, q\}$ is determined, the initial NARI coefficients are estimated by the method of least squares. In order to provide reliable results, the HRV processing techniques require uninterrupted series of R-R intervals. Nevertheless, peak-detection errors and ectopic beats often determine abrupt changes in the R-R interval series that may result in substantial deviations of the HRV indices, especially in changes in the dynamics. In addition, they could potentially bias the statistical outcomes. Therefore,

we preprocessed all the actual heartbeat data with a previously developed algorithm [54], also based on point process statistics, able to perform a real-time R-R interval error detection and correction.

D. Instantaneous Cardiovascular Assessment: Quantitative Tools

Our framework allows for three levels of quantitative characterization of heartbeat dynamics: instantaneous time-domain estimation, L power spectrum estimation, and HOS representation. The time-domain characterization is based on the first and the second-order moments of the underlying probability structure. Namely, given the time-varying parameter set $\boldsymbol{\xi}(t)$, the instantaneous estimates of mean R-R, R-R interval standard deviation, mean heart rate, and heart rate standard deviation can be extracted at each moment in time [39]. From $\xi(t)$, it is also possible to derive instantaneous quantitative tools such as the nth-order spectral representations. To summarize, the necessary steps are the following:

1) From the NL kernels $\gamma_n(\ldots)$ find the extended kernels $\gamma'_n(\ldots)$.
2) Compute the Fourier transforms $\Gamma'_n(\ldots)$ of the kernels $\gamma'_n(\ldots)$.
3) Compute the input–output Volterra kernels $H_k(\ldots)$ from the $\Gamma'_n(\ldots)$ of the autoregressive model.
4) Estimate the nth-order spectra such as the instantaneous spectrum $\mathcal{Q}(f,t)$ and bispectrum $\mathrm{Bis}(f_1,f_2,t)$.

Estimation of the Input–Output Volterra Kernels: As mentioned previously, the model quantitative tools are defined by means of the traditional input–output Wiener–Volterra coefficients. They are related to the Volterra series expansion and the Volterra theorem [55]. In functional analysis, a Volterra series denotes a functional expansion of a dynamic, NL, and time-invariant function and has been widely used in NL physiological modeling [56], [57]. The quadratic NARI model can be linked to the traditional input–output Volterra models by using a specific relationship [47] between the Fourier transforms of the Volterra kernels of order p, $H_p(f_1,\ldots,f_n)$, and the Fourier transforms of the extended NAR kernels, $\Gamma'_1(f_1)$ and $\Gamma'_2(f_1,f_2)$. In general, a second-order NARI model must be mapped in an infinite-order input–output Volterra model [47]:

$$\sum_{k=\mathrm{mid}(\rho)}^{\rho}\sum_{\sigma\in\sigma_\rho} H_k(f_{\sigma(1)},\ldots,f_{\sigma(r)},\omega_{\sigma(r+1)} + f_{\sigma(r+2)},\ldots,f_{\sigma(\rho-1)}+f_{\sigma(\rho)})\times\Gamma'_1(f_{\sigma(1)})\cdots\Gamma'_1(f_{\sigma(r)}) \times\Gamma'_2\left(f_{\sigma(r+1)},f_{\sigma(r+2)}\right)\cdots\Gamma'_2\left(f_{\sigma(\rho-1)},f_{\sigma(\rho)}\right)=0$$

where ρ is a given integer representing the kernel order, $\mathrm{mid}(\rho)=\lceil\rho/2\rceil$, $r=2k-\rho$, and σ_ρ is the permutation set of N_ρ. Obviously, there is the need to truncate the series to a reasonable order for actual application. In this study, we chose to model the cardiovascular activity with a cubic input–output Volterra by means of the following relationships with the NARI:

$$H_1(f)=\frac{1}{\Gamma'_1(f)} \tag{7}$$

$$H_2(f_1,f_2)=-\frac{\Gamma'_2(f_1,f_2)}{\Gamma'_1(f_1)\Gamma'_1(f_2)}\,H_1(f_1+f_2) \tag{8}$$

$$H_3(f_1,f_2,f_3)=-\frac{1}{6}\sum_{\sigma_3}\frac{\Gamma'_2\left(f_{\sigma_3(1)},f_{\sigma_3(2)}\right)}{\Gamma'_1\left(f_{\sigma_3(1)}\right)\Gamma'_1\left(f_{\sigma_3(2)}\right)} \times H_2\left(f_{\sigma_3(1)}+f_{\sigma_3(2)},f_{\sigma_3(3)}\right). \tag{9}$$

Instantaneous Spectral and Bispectral Analysis: The L power spectrum estimation reveals the L mechanisms governing the heartbeat dynamics in the frequency domain. In particular, given the input–output Volterra kernels of the NARI model for the instantaneous R-R interval mean $\mu_{\mathrm{RR}}(t,\mathcal{H}_t,\xi(t))$, we can compute the time-varying parametric (L) autospectrum [46] of the R-R intervals:

$$\mathcal{Q}(f,t)=2(1-\cos(\omega))S_{xx}(f,t)H_1(f,t)H_1(-f,t) -\frac{3}{2\pi}\int H_3(f,f_2,-f_2,t)S_{xx}(f_2,t)df_2 \tag{10}$$

where $S_{xx}(f,t)=\sigma^2_{\mathrm{RR}}$. By integrating the (10) in each frequency band, we can compute the indexes within the very low frequency (VLF = 0.01–0.04 Hz), low frequency (LF = 0.04–0.15 Hz), and high frequency (HF = 0.15–0.4 Hz) ranges.

The HOS representation allows for the consideration of statistics beyond the second order, and phase relations between frequency components otherwise suppressed [48], [58]. Higher order spectra (HOS), also known as polyspectra, are spectral representations of higher order statistics, i.e., moments and cumulants to the third order and beyond. HOS can detect deviations from linearity, stationarity, or Gaussianity. Particular cases of HOS is the third-order spectrum (Bispectrum), i.e., the Fourier transform of the third-order cumulant sequence [58]. As detailed next, Bispectrum is defined from the Volterra kernel coefficients estimated within the point process framework. Let $H_1(f)$ and $H_2(f_1,f_2,t)$ denote the Fourier transform of the first- and second-order Volterra kernel coefficients, respectively. The analytical solution for the bispectrum of a NL system response subject to stationary, zero-mean Gaussian input is [59]

$$\begin{aligned}\mathrm{Bis}(f_1,f_2,t)=&\,2H_2(f_1+f_2,-f_2,t)H_1(-f_1-f_2,t)H_1(f_2,t)\\ &\times\mathcal{S}_{xx}(f_1+f_2,t)\mathcal{S}_{xx}(f_2,t)+2H_2(f_1+f_2,-f_1,t)\\ &\times H_1(-f_1-f_2,t)H_1(f_1,t)\mathcal{S}_{xx}(f_1+f_2,t)\mathcal{S}_{xx}(f_1,t)\\ &+2H_2(-f_1,-f_2,t)H_1(f_1,t)H_1(f_2,t)\\ &\times\mathcal{S}_{xx}(f_1,t)\mathcal{S}_{xx}(f_2,t).\end{aligned} \tag{11}$$

The dynamic bispectrum is an important tool for evaluating the instantaneous presence of nonlinearity in time series [48], [60], [61]. Since the bispectrum presents several symmetry properties [58] dividing the (f_1,f_2) plane in eight symmetric zones, for a real signal it is uniquely defined by its values in the triangular region of computation Ω, $0\le f_1\le f_2\le f_1+f_2\le 1$. The sympatho-vagal L effects on the HRV are mainly characterized by the LF and HF spectral powers [37], [38]. Through

bispectral analysis, it is possible to further evaluate the nonlinear sympatho-vagal interactions by integrating $|B(f_1, f_2)|$ in the appropriate frequency bands. In particular, three bispectral measures, $\mathrm{LL}(t)$, $\mathrm{LH}(t)$, and $\mathrm{HH}(t)$, can be defined as:

$$\mathrm{LL}(t) = \int_{0.04}^{0.15}\int_{0.04}^{0.15} \mathrm{Bis}(f_1, f_2, t) df_1 df_2 \tag{12}$$

$$\mathrm{LH}(t) = \int_{0.04}^{0.15}\int_{0.15}^{0.4} \mathrm{Bis}(f_1, f_2, t) df_1 df_2 \tag{13}$$

$$\mathrm{HH}(t) = \int_{0.15}^{0.4}\int_{0.15}^{0.4} \mathrm{Bis}(f_1, f_2, t) df_1 df_2. \tag{14}$$

Equations (12) and (13) can be interpreted as indices of NL interaction between the sympathetic and the parasympathetic system, whereas (14) can be exclusively attributed to NL vagal dynamics.

E. Classification

The performance of the recognition of depressive and euthymic patterns was evaluated using a confusion matrix [62]. The generic element r_{ij} of the confusion matrix indicates the percentage of times a pattern belonging to the class i is classified as belonging to the class j. The training phase was carried out on 80% of the feature dataset, i.e., using no less than 16 min for each acquisition, while the testing phase was on the remaining 20%, i.e., using no less than 4 min for each acquisition. 4 min for each acquisition, with the constrain that each acquisition can be either considered as belonging to the training or test set. We performed a 40-fold cross-validation procedure [63]. In particular, for each of the 40 validation steps, the examples associated to the training and testing set are randomly chosen among all the available examples and results are described as mean and standard deviation among the 40 confusion matrices obtained. This procedure allows to obtain unbiased results on the recognition accuracy.

Multilayer Perceptron (MLP): We adopted the multilayer perceptron [64] with the integrate-and-fire neuron model for the representation of the relations between input and output values. We trained it by implementing a supervised learning method, i.e., input and output values are specified and the relations between them learnt. Specifically, in the training phase, for each data record, each activation function of the artificial neurons is calculated. The weight w_{ij} of a generic neuron i at the time T, for the input vector $\overline{f_n^k} = f_{n1}^k, \ldots, f_{nF}^k$ is modified on the basis of the well-established back propagation of the resulting error between the input and the output values. The response of the MLP is a boolean vector; each element represents the activation function of an output neuron. In this study, we implemented a MLP having three layers of neurons: input, hidden, and output layers. The input layer was formed by seven neurons, one for each of the feature space dimension. The hidden layer was constituted by an empirically estimated number of neurons. Specifically, we chose this number as the upper limit of the half difference between the number of the input and output neurons, i.e., 5. The output layer was formed by two neurons, one for each of the considered classes to be recognized.

TABLE I
CLINICAL LABELS ASSOCIATED TO EACH PATIENT DURING EACH ACQUISITION

ID	ACQ. 1	ACQ. 2	ACQ. 3	ACQ. 4	ACQ. 5
BP1	Euth				
BP2	Depr				
BP3	Depr	Euth			
BP4	Depr	Depr			
BP5	Depr	Depr	Depr	Depr	Euth
BP6	Depr	Depr	Euth		
BP7	Depr	Euth			
BP8	Depr	Euth			

III. EXPERIMENTAL PROTOCOLS

A. Recruitment of Eligible Subjects

Bipolar patients eligible for this study were chosen according to the following criteria: age 18–65, diagnosis of bipolar disorder (I or II), absence of suicidal tendencies, absence of delusions or hallucinations at the moment of recruitment, and absence of relevant somatic or neurological conditions. Details on patient acquisitions and associated mood states are reported in Table I. Patients were studied with an average frequency of two times a month. Each patient was evaluated and monitored from the day of the hospital admission toward remission, i.e., until the reaching of an euthymic state as long as such a condition was presented within three months after the first visit. All clinical states were evaluated by clinicians according to DSM-IV-TR criteria [65]. In this way, four possible clinical mood labels (depression, hypomania, mixed state, and euthymic state) were assigned. The mood label associated with each patients evaluation was assigned independently with respect to the previous ones. Euthymic state, i.e., clinical remission was defined by having a score below threshold on a quantitative psychopathological rating scale (for depressive symptoms, score below 8 on the 16-item Quick Inventory of Depressive Symptomatology Clinician Rating and for manic symptoms score below 6 on the Young Mania Rating Scale). The same thresholds were also used to define a change in mood state. No data selection criteria were used to choose the time window. A physician presented the study to each patient. Before entering the study, each patient signed an informed consent approved by the ethical committee of the University of Pisa. Once enrolled, the patients were administered a set of questionnaires and rating scales in order to assess the current mood. Clinicians associated a mood label in agreement with one of the five possible defined mood states: euthymia, depression, mania, hypomania, and mixed state.

B. Affective Elicitation Protocol

Patients BP1, BP2, BP3, BP4, and BP5 underwent a dedicated affective elicitation protocol which started with two, 5-min phases in resting state with eyes closed and open. Subsequently, passive (international affective picture system (IAPS) [66]), lasting for 6 min, and active (thematic apperception test (TAT) [67]), lasting for at least 2 min, visual stimuli were administered. Finally, in order to provide a common point of reference, patients were asked to recite a paragraph from the Universal Declaration of Human Rights lasting two more minutes. The IAPS database

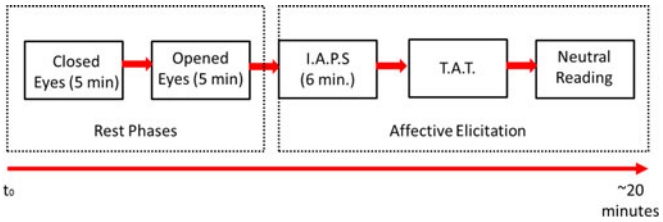

Fig. 2. Timeline of the affective elicitation protocol.

consists of hundreds of pictures tagged by specific emotional ratings in terms of valence, arousal, and dominance. The protocol implies a slideshow of pictures having two classes of arousal, either minimum or maximum, and random valence, ranging from unpleasant to pleasant. After IAPS elicitation, the patients were asked to describe several TAT images. The TAT, a projective psychological test, is supposed to tap the subject's subconscious and reveal repressed aspects of personality, motives and needs for achievement, power and intimacy, and problem-solving skills. However, in this protocol, the pictures were only used to elicit spontaneous comments from the patients. Of note, as there is no standardization of the use of the texts/pictures according to the subjects' clinical state, text/picture stimuli were always proposed in the same order. A schematic timeline of the experimental protocol is shown in Fig. 2.

C. Unstructured Activity

In order to study the capability of the proposed NARI methodology in generalizing the recognition of depressive and euthymic patterns of bipolar patients on the experimental protocol, we further studied three bipolar patients (i.e., BP6, BP7, and BP8) who were asked to wear the PSYCHE wearable monitoring platform at all times until the battery ran out, i.e., approximately 18 h. Therefore, there was no need of particular experimental conditions as the patient was free to perform normal activities. Here, we analyzed a smaller part of these long-term acquisitions in order to study the same amount of data with respect to the first affective elicitation protocol. Therefore, no less than 20 min of heartbeat dynamics gathered during unknown (unstructured) activities were taken into account.

D. Analysis Overview

We analyzed eight bipolar patients having depressive and euthymic states. ECG was acquired by using the PSYCHE platform and R-R interval series were extracted and analyzed by the NARI model to obtain the cardiovascular indices. Then, a set of features extracted from the L and the NL kernels was used to implement the automatic mood-tracking system. Experimental results are shown in terms of statistical inference and confusion matrices [62]. A comparative study considering the same features extracted using standard signal processing techniques was further performed. Classification performances encompass both experimental protocols.

We considered the median values over the estimated instantaneous time series according to the protocol timeline. All ranges reported in this study are expressed as median and its respective absolute deviation (i.e., for a feature X, we report $\text{Median}(X) \pm \text{MAD}(X)$ where $\text{MAD}(X) = \text{Median}(|X - \text{Median}(X)|)$).

IV. Results

For each subject, the NARI model was applied to the R-R series detected from the recorded ECG. The optimal model order was chosen by means of the Akaike information criterion (AIC) [39] applied to the first 5-min R-R recordings. The AIC analysis indicated $6 \leq p \leq 8$ and $1 \leq q \leq 2$ as optimal orders. All the KS distances were <0.06 and no less than 97% of the autocorrelation points were inside the boundaries. The L and NL indices, described in Section II-B, were evaluated for all available recordings. The instantaneous identification (5-ms resolution) was averaged within a time window of 1 s. Representative tracking results are shown in Fig. 3 for BP1 (euthymic phase, top) and BP2 (depressive phase, bottom).

A preliminary statistical analysis was performed in order to evaluate the intrasubject contribution of each feature. Statistical inferences were performed to test the null hypothesis of no significative differences occurring among different mood states. Such analyses were performed on patients undergoing the affective elicitation protocol and having more than one acquisition, i.e., BP3, BP4, and BP5. First, the whole feature pattern (L and NL) was treated as multivariate distribution and tested by means of nonparametric multivariate analysis of variance (npMANOVA). Such a test revealed statistical differences among acquisitions for all the three patients (BP3: $p < 10^{-6}$; BP4: $p < 0.005$; BP5: $p < 10^{-6}$). No significant conclusions can be drawn from this analysis, which is therefore insufficient for an effective discriminative task. As a consequence, further monovariate statistical analyses were performed to evaluate the difference among acquisitions for each of the extracted features. Nonparametric Kruskal–Wallis and Rank-Sum tests were used to investigate the intersubject variability among the five acquisitions of BP5 and the two acquisitions of BP3 and BP4, respectively. These results are summarized in Tables II, III, and IV. All of the features coming from the L and NL coefficients were taken into account. We obtained significative p-values in all cases but the LF/HF ratio of BP4. Remarkably, this is the only patient having more than one acquisition with the same mood label. Moreover, an intersubject analysis was performed to reveal the mood pattern, which would be in common among patients. Discrimination of the mood states was performed using the well-known MLP neural network [64]. All results are expressed in the form of confusion matrix, after 40-fold cross validation.

For each experimental protocol (affective elicitation and unstructured activity), we compared the MLP accuracy by creating two feature sets. The first set, α, is composed by $\mu_{\text{RR}}(t, \mathcal{H}_t, \xi(t))$, σ_{RR}, and the spectral indices LF, HF, and LF/HF. In other words, the feature set α comes from the L terms of the model. The second set, β, includes the NL LL,

TABLE II
RESULTS FOR THE INTRASUBJECT EUTHYMIA-DEPRESSION DISCRIMINATION

BP5	Derivation	ACQ1 (Depr)	ACQ2 (Depr)	ACQ3 (Depr)	ACQ4 (Depr)	ACQ5 (Euth)	P-val
μ_{RR}(ms)	L-NL	708.46±6.47	764.01±11.47	733.67±13.94	660.95±14.45	590.86±6.93	$< 10^{-6}$
σ_{RR}(ms)	L-NL	31.82±7.07	47.13±13.09	84.59±29.12	22.74±5.82	15.28±3.67	$< 10^{-6}$
$LF(ms^2)$	L	21.56±15.29	40.80±34.84	28.49±27.96	2.38±2.05	1.51±0.89	$< 10^{-6}$
$HF(ms^2)$	L	12.37±7.88	23.41±12.32	36.28±18.85	6.88±3.11	4.75±2.17	$< 10^{-6}$
LF/HF	L	1.01±0.81	1.60±1.29	0.69±0.65	0.40±0.30	0.41±0.21	$< 10^{-6}$
$LL\ (10^6)$	NL	10.32±8.94	42.85±36.54	29.73±26.34	2.85±2.05	1.23±0.76	$< 10^{-6}$
$LH\ (10^6)$	NL	28.20±20.06	61.78±44.17	73.22±50.80	17.87±11.98	5.43±3.46	$< 10^{-6}$
$HH\ (10^6)$	NL	104.27±68.47	117.11±75.44	140.95±81.53	90.81±54.20	31.89±16.26	$< 10^{-6}$

P-values are obtained from the Kruskal-Wallis test.

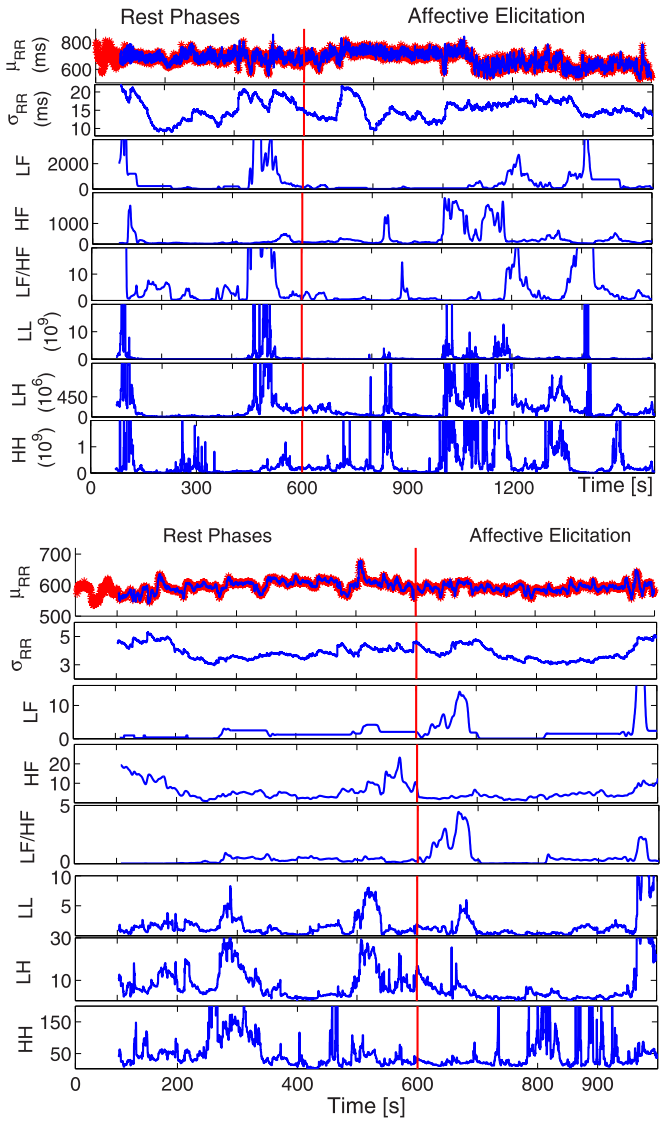

Fig. 3. Instantaneous HRV statistics computed from Subject 1 (top) and Subject 2 (bottom) during the euthymic and depressive state, respectively. The estimated $\mu_{\mathrm{RR}}(t, \mathcal{H}_t, \xi(t))$ is superimposed on the recorded R-R series. Following next, the instantaneous heartbeat standard deviation, the instantaneous heartbeat spectral LF, and HF powers and their ratio. Finally, bottom rows report on the three bispectral statistics.

TABLE III
RESULTS FOR THE INTRASUBJECT EUTHYMIA-DEPRESSION DISCRIMINATION

BP4	Derivation	ACQ1 (Depr)	ACQ2 (Depr)	P-val
μ_{RR}(ms)	L-NL	734.46±15.94	655.34±5.92	$< 10^{-6}$
σ_{RR}(ms)	L-NL	146.39±67.50	39.86±7.62	$< 10^{-6}$
$LF(ms^2)$	L	197.54±186.57	23.90±18.67	$< 10^{-6}$
$HF(ms^2)$	L	53.42±30.45	18.47±9.49	$< 10^{-6}$
LF/HF	L	3.16±2.86	1.29±1.16	> 0.05
$LL\ (10^6)$	NL	65.83±53.67	17.35±11.52	$< 10^{-6}$
$LH\ (10^6)$	NL	83.46±58.22	75.44±34.19	$< 10^{-6}$
$HH\ (10^6)$	NL	121.09±64.45	124.64±71.65	$< 10^{-6}$

P-values are obtained from the Rank-Sum test.

TABLE IV
RESULTS FOR THE INTRASUBJECT EUTHYMIA-DEPRESSION DISCRIMINATION

BP3	Derivation	ACQ1 (Depr)	ACQ2 (Euth)	P-val
μ_{RR}(ms)	L-NL	632.61±9.44	628.13±18.84	$< 10^{-6}$
σ_{RR}(ms)	L-NL	304.79±97.86	237.73±104.25	$< 10^{-6}$
$LF(ms^2)$	L	11.45±10.14	104.77±86.99	$< 10^{-6}$
$HF(ms^2)$	L	42.69±21.98	107.00±53.63	$< 10^{-6}$
LF/HF	L	0.27±0.23	0.99±0.75	$< 10^{-6}$
$LL\ (10^6)$	NL	3.92±2.92	35.54±27.75	$< 10^{-6}$
$LH\ (10^6)$	NL	12.61±9.88	83.34±48.59	$< 10^{-6}$
$HH\ (10^6)$	NL	67.53±48.78	136.46±73.80	$< 10^{-6}$

P-values are obtained from the Rank-Sum test.

LH, and HH indices which will be joined to the α set for future evaluations.

A. *Affective Elicitation Protocol*

In this section, the results of the classification using data gathered from patients undergoing the affective elicitation protocol (i.e., BP1, BP2, BP3, BP4, and BP5), are reported. In order to take into account the imbalanced number of available examples per class, two different learning rates were considered in the MLP training phases giving the euthymic examples three times more penalty with respect to the depressive examples. The MLP results using the NARI model are summarized in Table V. It shows the recognition accuracy by considering all five patients. Using dataset α, correct recognition of the euthymic state is below 75%, whereas accuracy increases up to 99% using dataset $\alpha + \beta$. To further justify the instantaneous point-process NARI approach, we estimated the L and NL features of the α and β sets by means of standard AR models [68] and then tested the MLP capability of mood discrimination. The relative confusion matrices are shown in Table VI. In this case, neither using

TABLE V
RESULTS FOR THE INTERSUBJECT EUTHYMIA-DEPRESSION DISCRIMINATION IN PATIENTS BP1, BP2, BP3, BP4, AND BP5 USING THE POINT PROCESS NARI MODEL

MLP-5 Patients	Dataset	**Euthymia**	**Depression**
Euthymia	α	74.44 $\pm$ 18.21	1.09 $\pm$ 1.92
	$\alpha+\beta$	**99.56 $\pm$ 0.39**	0.01 $\pm$ 0.06
Depression	α	25.55 $\pm$ 18.21	98.91 $\pm$ 1.92
	$\alpha+\beta$	0.44 $\pm$ 0.40	**99.98 $\pm$ 0.06**

Bold indicates the best classification accuracy for each class.

TABLE VI
RESULTS FOR THE INTERSUBJECT EUTHYMIA-DEPRESSION DISCRIMINATION IN PATIENTS BP1, BP2, BP3, BP4, AND BP5 USING STANDARD BIOSIGNAL PROCESSING TECHNIQUES

MLP-5 Patients	Dataset	**Euthymia**	**Depression**
Euthymia	α	25.00 $\pm$ 25.32	15.50 $\pm$ 16.00
	$\alpha+\beta$	32.50 $\pm$ 31.11	21.50 $\pm$19.42
Depression	α	75.00 $\pm$ 25.32	84.50 $\pm$16.00
	$\alpha+\beta$	67.50 $\pm$ 31.11	78.50 $\pm$19.42

TABLE VII
RESULTS FOR THE INTERSUBJECT EUTHYMIA-DEPRESSION DISCRIMINATION IN PATIENTS BP6, BP7, AND BP8 USING THE POINT PROCESS NARI MODEL

MLP-3 Patients	Dataset	**Euthymia**	**Depression**
Euthymia	α	60.36 $\pm$ 18.35	14.34 $\pm$ 7.80
	$\alpha+\beta$	**82.38 $\pm$ 14.97**	13.88 $\pm$ 10.99
Depression	α	39.64 $\pm$ 18.35	85.66 $\pm$ 7.80
	$\alpha+\beta$	17.60 $\pm$ 14.99	**86.12 $\pm$ 10.99**

Bold indicates the best classification accuracy for each class.

the α feature set nor using the joined $\alpha+\beta$ set, a sufficient satisfactory recognition was reached.

B. Unstructured Activity

In this section, the results of the classification using data gathered from patients performing unstructured activity (i.e., BP6, BP7, and BP8), are reported. MLP results using the NARI model are summarized in Table VII. It shows the recognition accuracy by considering all three patients. Using dataset α, correct recognition of the euthymic state is below 61%, whereas accuracy increases up to 82.38% using the feature set $\alpha+\beta$, i.e., considering the instantaneous NL cardiovascular dynamics.

C. Joined Dataset

In order to investigate whether common patterns of heartbeat L and NL dynamics exist between euthymia and depressive states regardless of the experimental protocol/elicitation, we performed the intersubject euthymia-depression classification using data gathered from all patients. The two datasets representing instantaneous cardiovascular dynamics in bipolar patients during affective elicitation protocol and unstructured activity were joined. The classification results are shown in Table VIII, which also confirms the crucial role of heartbeat NL dynamics in pathological mood states. When processing the feature set $\alpha+\beta$, in fact, the recognition accuracy dramatically increases, and the corresponding average accuracy is beyond 90%.

TABLE VIII
RESULTS FOR THE INTERSUBJECT EUTHYMIA-DEPRESSION DISCRIMINATION ON ALL EIGHT PATIENTS USING THE POINT PROCESS NARI MODEL

MLP-8 Patients	Dataset	**Euthymia**	**Depression**
Euthymia	α	43.40 $\pm$ 20.83	2.21 $\pm$ 2.61
	$\alpha+\beta$	**91.06 $\pm$ 6.02**	2.46 $\pm$ 1.74
Depression	α	56.60 $\pm$ 20.83	**97.79 $\pm$ 2.61**
	$\alpha+\beta$	8.94 $\pm$ 6.02	97.54 $\pm$ 1.74

Bold indicates the best classification accuracy for each class.

V. DISCUSSION AND CONCLUSION

In both normal psychology and psychopathology, mood is considered quite a stable characteristic of the individual affective dimension, while emotions are considered transient, acute, and arousing responses to specific environmental stimuli. However, it is very well documented both in clinical experience and in research studies that mood affects emotions, emotional regulation, and emotional response. For this reason, a possible approach to investigate mood recognition is to explore emotional changes provoked by external stimuli. Accordingly, along the conceptual rationale behind the PSYCHE project, we have proposed a novel system along with an experimental/methodological approach for the assessment of instantaneous ANS patterns of depression in bipolar patients. The use of ANS dynamics represents a reasonable way to explore neurobiological and psychophysiological correlates of mood disorders. The feasibility of this approach has been documented in other research articles both for depression and bipolar disorders [15]–[18], [69], [70]. For instance, Levy [71] showed a higher ANS activation in bipolar patients as compared to controls and linked chronic ANS arousal to neurodegeneration and toxiticty. It is also well known that emotional modulation techniques (used in the psychotherapy of mental disorders) modulates ANS activity [72], [73]. Finally, vagal nerve stimulation is currently used as treatment for refractory depression [74] based on the fact that a boost of parasympathetic activity can modulate positive mood. All of these research points to a link between ANS dynamics and bipolar disorders, i.e., links the peripheral nervous system to a disorder of the central nervous system. In-depth psychophysiological reasons of such a link are still debated, although few hypotheses can be drawn. In particular, it is important to note that the ANS is indirectly affected by central nervous system activity: Anxiety, fear, disgust, and the other primary emotions have both central and peripheral correlates. For instance, the central activity of some brain structures such as amygdala, anterior cingulate, hypothalamus, ventromedial prefrontal cortex can directly affect ANS discharge through the modulation of sympathetic and vagal nuclei of the brain stem [75], [76]. We believe that since this modulation is present in healthy subjects, it is also present in an anomalous way in patients with mood disorders and dysfunctions of emotion expressions and regulations [77].

The proposed approach allows the mathematical representation of the cardiovascular system as a NL dynamical system characterized by means of a "perturbation" analysis, i.e, analysis before and after short-time emotional elicitation. In order to show a preliminary validation of the proposed methodologies,

we analyzed data coming from five patients experiencing depressive and euthymic episodes, and enrolled them to participate in dedicated affective elicitation protocol. Furthermore, data from three bipolar patients while performing unlabeled and unstructured normal activities were taken into account. In both cases, a comfortable, textile-based sensorized t-shirt (namely the PSYCHE platform) was used to perform noninvasive recordings of physiological variables, and a novel point-process NARI model was implemented and applied to the R-R series derived from the ECG in order to produce novel instantaneous features. In particular, standard features in both the time (i.e., $\mu_{\mathrm{RR}}(t, \mathcal{H}_t, \xi(t))$ and σ_{RR}), and frequency domain (i.e., LF, HF, and LF/HF) along with higher order NL features, i.e., LL, LH, and HH, were extracted from the processed R-R series. The NARI model was used to characterize the mean of an IG distribution representing the interbeat probability function. Such an approach allows for the instantaneous estimation of all HRV measures without any interpolation method [39]. The method is also personalized, fully parametric, and able to improve nonstationary identification [46].

All of the mentioned features coming from the NARI representation of the heartbeat dynamics were investigated by using statistical inference and pattern recognition methods in intra- and intersubject analyses, respectively. Multivariate statistical analysis by using an npMANOVA approach on patients undergoing the affective elicitation protocol revealed significant within subject differences among different mood states, whereas monovariate analyses pointed out that only the LF/HF is statistically similar between two depressive phases. Pattern recognition algorithms (MLP) were then applied to the estimated features to classify the mood state of the patients (i.e., "euthymia" or "depression"), and two feature sets were compared. The first set, α, was comprised of only the standard feature set, whereas the NL indices were added to the second set, β. We performed a comparative classification analysis in order to evaluate the role of the NL dynamics on the intersubject variability. Considering the dataset comprised of data coming from the five patients emotionally elicited, a classification accuracy of up to about 74% for the α (L) set, and up to about 99% for the $\alpha + \beta$ (L and NL) set was achieved for the euthymic class (see Table V). Therefore, it is clear that the high-intersubject variability strongly affects the information given by the L contribution (set α) of the model whereas it does not affect the NL one (set $\alpha + \beta$). A further comparison analysis using traditional signal processing techniques revealed that noninstantaneous information was not sufficient for a reliable assessment (see Table VI). The crucial role of NL dynamics for the characterization of depressive states in bipolar patients was also confirmed when testing the capability of the proposed methodology with data gathered from unstructured activities (see Tables VII and VIII).

Our results demonstrate that a common pattern of instantaneous heartbeat features can be found despite the intersubject variability and experimental protocol undertaken. Our results also show that the inclusion of NL indices gives improved results and smaller variance with respect to the classification performed by only using the standard features. The results obtained using data gathered during the affective elicitation protocol (99.56% accuracy) went beyond expectations, also considering that the few misclassified samples can be easily interpreted as either algorithmic/mathematical artifacts or physiological outliers, i.e., events not related to mood markers for whatever reason. On the other hand, we expected a lower classification accuracy using data coming from unstructured activity. Moreover, it is possible to hypothesize that the altered ANS dynamics related to pathological mental states, modulated by the central functional structures of the brain, can be revealed without particular experimental conditions and using NARI point-process models. However, structured emotional relevant experimental conditions can contribute in increasing the accuracy of the system. It is worthwhile mentioning that the chosen affective elicitation protocol does not strictly require a wearable monitoring system to acquire ANS data. However, a comfortable monitoring system dramatically increases the patient's compliance and improves the reliability of the physiological variations, which are instantaneously detected by the proposed NARI model. Such an experimental procedure is part of a more comprehensive study involving long-term monitoring of bipolar patients in naturalistic environments [15]–[18], [78], i.e., the unstructured activity analysis.

The presented point-process NL analysis represents a pioneering study in the field of mood assessment in bipolar patients. In our approach, we consider the acquisition paradigm (including high and low arousing IAPS and TAT) as a whole, without subdividing the protocol in separate epochs. More than a limitation, we consider that the overall results give additional strength to our approach. Indeed, it is not a matter of specific emotional response but, more in general, the central issue is the reactivity of the ANS to be affected in bipolar disorders. The fact that we were able to detect changes in ANS during the protocol as compared to a resting state baseline is enough to say that we are studying ANS reactions despite subjective measurements of emotional arousal or valence related to the cues we used. Future studies will progress to increasing the number of patients enrolled in order to confirm the reliability of the proposed approach. We will also explore additional aspects of the L and NL identification as related to depression and other pathological states of the bipolar disorder. Moreover, we will carefully explore the physiological meaning of the dynamic autonomic signatures both in the context of the underlying mood state and as a result of the different stimuli administered within the dedicated protocol. Our approach will be also further extended within the PSYCHE project, including several other available variables (e.g., voice, activity index, sleep pattern alteration, electrodermal response, and biochemical markers).

ACKNOWLEDGMENT

The authors are grateful to L. Maley for carefully reviewing the paper.

REFERENCES

[1] R. C. Kessler, K. A. McGonagle, S. Zhao, C. B. Nelson, M. Hughes, S. Eshleman, H. Wittchen, and K. S. Kendler, "Lifetime and 12-month prevalence of DSM-III-R psychiatric disorders in the united states: results

from the national comorbidity survey," *Archives Gen. Psychiatry*, vol. 51, no. 1, pp. 8–19, 1994.
[2] H. Wittchen and F. Jacobi, "Size and burden of mental disorders in europe–a critical review and appraisal of 27 studies," *Eur. Neuropsychopharmacol.*, vol. 15, no. 4, pp. 357–376, 2005.
[3] E. Vieta, M. Reinares, and A. Rosa, "Staging bipolar disorder," *Neurotoxicity Res.*, vol. 19, no. 2, pp. 279–285, 2011.
[4] A. Andreazza, M. Kauer-Sant'Anna, B. Frey, D. Bond, F. Kapczinski, L. Young, and L. Yatham, "Oxidative stress markers in bipolar disorder: a meta-analysis," *J. Affective Disorders*, vol. 111, no. 2, pp. 135–144, 2008.
[5] H. Stampfer, "The relationship between psychiatric illness and the circadian pattern of heart rate," *Australasian Psychiatry*, vol. 32, no. 2, pp. 187–198, 1998.
[6] G. Iverson, H. Stampfer, and M. Gaetz, "Reliability of circadian heart pattern analysis in psychiatry," *Psychiatric Quart.*, vol. 73, no. 3, pp. 195–203, 2002.
[7] G. Iverson, M. Gaetz, E. Rzempoluck, P. McLean, W. Linden, and R. Remick, "A new potential marker for abnormal cardiac physiology in depression," *J. Behavioral Med.*, vol. 28, no. 6, pp. 507–511, 2005.
[8] J. Taillard, P. Sanchez, P. Lemoine, and J. Mouret, "Heart rate orcadian rhythm as a biological marker of desynchronization in major depression: A methodological and preliminary report," *Chronobiol. Int.*, vol. 7, no. 4, pp. 305–316, 1990.
[9] J. Taillard *et al.*, "Sleep and heart rate circadian rhythm in depression: The necessity to separate," *Chronobiol. Int.*, vol. 10, no. 1, pp. 63–72, 1993.
[10] R. Carney, K. Freedland, M. Rich, and A. Jaffe, "Depression as a risk factor for cardiac events in established coronary heart disease: A review of possible mechanisms," *Ann. Behavioral Med.*, vol. 17, no. 2, pp. 142–149, 1995.
[11] A. Glassman, "Depression, cardiac death, and the central nervous system," *Neuropsychobiology*, vol. 37, no. 2, pp. 80–83, 1998.
[12] L. Watkins, J. Blumenthal, and R. Carney, "Association of anxiety with reduced baroreflex cardiac control in patients after acute myocardial infarction," *Amer. Heart J.*, vol. 143, no. 3, pp. 460–466, 2002.
[13] A. Fagiolini, K. Chengappa, I. Soreca, and J. Chang, "Bipolar disorder and the metabolic syndrome: Causal factors, psychiatric outcomes and economic burden," *CNS Drugs*, vol. 22, no. 8, pp. 655–669, 2008.
[14] K. Latalova, J. Prasko, T. Diveky, A. Grambal, D. Kamaradova, H. Velartova, J. Salinger, and J. Opavsky, "Autonomic nervous system in euthymic patients with bipolar affective disorder," *Neuro Endocrinol. Lett.*, vol. 31, no. 6, pp. 829–836, 2010.
[15] G. Valenza, M. Nardelli, A. Lanata, C. Gentili, G. Bertschy, R. Paradiso, and E. Scilingo, "Wearable monitoring for mood recognition in bipolar disorder based on history-dependent long-term heart rate variability analysis," *IEEE J. Biomed. Health Informat.*, to be published.
[16] A. Greco, G. Valenza, A. Lanata, G. Rota, and E. Scilingo, "Electrodermal activity in bipolar patients during affective elicitation," *IEEE J. Biomed. Health Informat.*, to be published.
[17] G. Valenza, C. Gentili, A. Lanatà, and E. P. Scilingo, "Mood recognition in bipolar patients through the psyche platform: Preliminary evaluations and perspectives," *Artif. Intell. Med.*, vol. 57, no. 1, pp. 49–58, 2013.
[18] N. Vanello, A. Guidi, C. Gentili, S. Werner, G. Bertschy, G. Valenza, A. Lanata, and E. P. Scilingo, "Speech analysis for mood state characterization in bipolar patients," in *Proc. Eng. Med. Biol. Soc Annu. Int. Conf. IEEE*, 2012, pp. 2104–2107.
[19] E. Scilingo, A. Gemignani, R. Paradiso, N. Taccini, B. Ghelarducci, and D. De Rossi, "Performance evaluation of sensing fabrics for monitoring physiological and biomechanical variables," *IEEE Trans. Inf. Technol. Biomed.*, vol. 9, no. 3, pp. 345–352, Sep. 2005.
[20] M. Di Rienzo, P. Meriggi, F. Rizzo, P. Castiglioni, C. Lombardi, M. Ferratini, and G. Parati, "Textile technology for the vital signs monitoring in telemedicine and extreme environments," *IEEE Trans., Inf. Technol. Biomed.*, vol. 14, no. 3, pp. 711–717, May 2010.
[21] E. Jovanov, A. O'Donnel, A. Morgan, B. Priddy, and R. Hormigo, "Prolonged telemetric monitoring of heart rate variability using wireless intelligent sensors and a mobile gateway," in *Proc. IEEE Eng. Biol. Med. Conf.*, 2002, vol. 3, pp. 1875–1876.
[22] P. Bonato, "Wearable sensors/systems and their impact on biomedical engineering," *IEEE Eng. Med. Biol. Mag.*, vol. 22, no. 3, pp. 18–20, May/Jun. 2003.
[23] A. Lanata, G. Valenza, and E. Scilingo, "A novel EDA glove based on textile-integrated electrodes for affective computing," *Med. Biol. Eng. Comput.*, vol. 50, pp. 1–10, 2012.
[24] G. Valenza, A. Lanatà, E. P. Scilingo, and D. De Rossi, "Towards a smart glove: Arousal recognition based on textile electrodermal response," in *Proc. IEEE Eng. Biol. Med. Conf.*, 2010, pp. 3598–3601.
[25] S. Johnson, J. Gruber, and L. Eisner, "Emotion and bipolar disorder" 2007.
[26] G. Valenza, A. Lanatá, and E. P. Scilingo, "Improving emotion recognition systems by embedding cardiorespiratory coupling," *Physiol. Meas.*, vol. 34, no. 4, pp. 449–464, 2013.
[27] G. Valenza, L. Citi, A. Lanata, E. P. Scilingo, and R. Barbieri, "A nonlinear heartbeat dynamics model approach for personalized emotion recognition," in *Proc. IEEE Eng. Biol. Med. Conf.*, 2013, pp. 2579–2582.
[28] G. Valenza, A. Lanata, and E. P. Scilingo, "Oscillations of heart rate and respiration synchronize during affective visual stimulation," *IEEE Trans. Inf. Technol. Biomed.*, vol. 16, no. 4, pp. 683–690, Jul. 2012.
[29] G. Valenza, A. Lanata, and E. P. Scilingo, "The role of nonlinear dynamics in affective valence and arousal recognition," *IEEE Trans. Affective Comput.*, vol. 3, no. 2, pp. 237–249, Apr./Jun. 2012.
[30] M. Swangnetr and D. B. Kaber, "Emotional state classification in patient–robot interaction using wavelet analysis and statistics-based feature selection," *IEEE Trans. Human-Mach. Syst.*, vol. 43, no. 1, pp. 63–75, Jan. 2013.
[31] G. Valenza, P. Allegrini, A. Lanatà, and E. P. Scilingo, "Dominant Lyapunov exponent and approximate entropy in heart rate variability during emotional visual elicitation," *Frontiers Neuroeng.*, vol. 5, pp. 1–7, 2012.
[32] R. A. Calvo and S. D'Mello, "Affect detection: An interdisciplinary review of models, methods, and their applications," *IEEE Trans. Affective Comput.*, vol. 1, no. 1, pp. 18–37, Jan. 2010.
[33] M. Orini, R. Bailón, R. Enk, S. Koelsch, L. Mainardi, and P. Laguna, "A method for continuously assessing the autonomic response to music-induced emotions through HRV analysis," *Med. Biol. Eng. Comput.*, vol. 48, no. 5, pp. 423–433, 2010.
[34] L. Wang, K. LaBar, and G. McCarthy, "Mood alters amygdala activation to sad distractors during an attentional task," *Biol. Psychiatry*, vol. 60, no. 10, pp. 1139–1146, 2006.
[35] D. Radaelli, S. Poletti, S. Dallaspezia, C. Colombo, E. Smeraldi, and F. Benedetti, "Neural responses to emotional stimuli in comorbid borderline personality disorder and bipolar depression," *Psychiatry Res.*, vol. 203, pp. 61–66, 2012.
[36] A. Greco, A. Lanata, G. Valenza, G. Rota, N. Vanello, and E. Scilingo, "On the deconvolution analysis of electrodermal activity in bipolar patients," in *Proc. IEEE Eng. Biol. Med. Conf.*, 2012, pp. 6691–6694.
[37] T. F. of the European Society of Cardiology, the North American Society of Pacing, and Electrophysiology, "Heart rate variability: Standards of measurement, physiological interpretation and clinical use," *Circulation*, vol. 93, no. 5, pp. 1043–65, 1996.
[38] U. Rajendra Acharya, K. Paul Joseph, N. Kannathal, C. Lim, and J. Suri, "Heart rate variability: A review," *Med. Biol. Eng. Comput.*, vol. 44, no. 12, pp. 1031–1051, 2006.
[39] R. Barbieri, E. C. Matten, A. A. Alabi, and E. N. Brown, "A point-process model of human heartbeat intervals: new definitions of heart rate and heart rate variability," *Amer. J. Physiol.-Heart Circ. Physiol.*, vol. 288, no. 1, pp. H424–H435, 2005.
[40] R. Barbieri and E. Brown, "Analysis of heartbeat dynamics by point process adaptive filtering," *IEEE Trans. Biomed. Eng.*, vol. 53, no. 1, pp. 4–12, Jan. 2006.
[41] Z. Chen, E. Brown, and R. Barbieri, "Assessment of autonomic control and respiratory sinus arrhythmia using point process models of human heart beat dynamics," *IEEE Trans. Biomed. Eng.*, vol. 56, no. 7, pp. 1791–1802, Jul. 2009.
[42] Z. Chen, E. Brown, and R. Barbieri, "Characterizing nonlinear heartbeat dynamics within a point process framework," *IEEE Trans. Biomed. Eng.*, vol. 57, no. 6, pp. 1335–1347, Jun. 2010.
[43] G. Valenza, L. Citi, E. Scilingo, and R. Barbieri, "Point-process nonlinear models with Laguerre and Volterra expansions: Instantaneous assessment of heartbeat dynamics," *IEEE Trans. Signal Process.*, vol. 61, no. 11, pp. 2914–2926, Jun. 2013.
[44] G. Valenza, L. Citi, E. Scilingo, and R. Barbieri, "Instantaneous bispectral characterization of the autonomic nervous system through a point-process nonlinear model," in *World Congress on Medical Physics and Biomedical Engineering*. Berlin, Germany: Springer, 2013, pp. 530–533.
[45] G. Valenza, L. Citi, and R. Barbieri, "Instantaneous nonlinear assessment of complex cardiovascular dynamics by Laguerre-Volterra point process models," in *Proc. IEEE Eng. Biol. Med. Conf.*, 2013, pp. 6131–6134.
[46] C. W. J. Granger and R. Joyeux, "An introduction to long-memory time series models and fractional differencing," *J. Time Series Anal.*, vol. 1, no. 1, pp. 15–29, 1980.

[47] J. Le Caillec and R. Garello, "Nonlinear system identification using autoregressive quadratic models," *Signal Process.*, vol. 81, no. 2, pp. 357–379, 2001.
[48] C. Nikias and J. Mendel, "Signal processing with higher-order spectra," *IEEE Signal Process. Mag.*, vol. 10, no. 3, pp. 10–37, Jul. 1993.
[49] K. Sunagawa, T. Kawada, and T. Nakahara, "Dynamic nonlinear Vago-sympathetic interaction in regulating heart rate," *Heart Vessels*, vol. 13, no. 4, pp. 157–174, 1998.
[50] J. Mendel, "Tutorial on higher-order statistics (spectra) in signal processing and system theory: Theoretical results and some applications," *Proc. IEEE*, vol. 79, no. 3, pp. 278–305, Mar. 1991.
[51] C. Nikias, *Higher-order Spectral Analysis: A Nonlinear Signal Processing Framework*. Englewood Cliffs, NJ, USA: Prentice-Hall, 1993.
[52] Z. Chen, P. Purdon, E. Brown, and R. Barbieri, "A differential autoregressive modeling approach within a point process framework for non-stationary heartbeat intervals analysis," in *Proc. IEEE Eng. Biol. Med. Conf.*, 2010, pp. 3567–3570.
[53] C. Loader, *Local Regression and Likelihood*. New York, NY, USA: Springer-Verlag, 1999.
[54] L. Citi, E. Brown, and R. Barbieri, "A real-time automated point process method for detection and correction of erroneous and ectopic heartbeats," *IEEE Trans. Biomed. Eng.*, vol. 59, no. 10, pp. 2828–2837, Oct. 2012.
[55] S. Billings, "Identification of nonlinear system—A survey," *Proc. IEEE*, vol. 127, no. 6, pp. 272–285, Nov. 1980.
[56] M. Akay, *Nonlinear Biomedical Signal Processing Vol. II: Dynamic Analysis and Modeling*. New York, NY, USA: Wiley, 2000.
[57] V. Marmarelis, "Modeling of neuronal systems," in *Nonlinear Dynamic Modeling of Physiological Systems*. New York, NY, USA: Wiley, 2012, pp. 407–465.
[58] C. Nikias and M. Raghuveer, "Bispectrum estimation: A digital signal processing framework," *Proc. IEEE*, vol. 75, no. 7, pp. 869–891, Jul. 1987.
[59] J. M. Nichols, C. C. Olson, J. V. Michalowicz, and F. Bucholtz, "The bispectrum and bicoherence for quadratically nonlinear systems subject to non-Gaussian inputs," *IEEE Trans. Signal Process.*, vol. 57, no. 10, pp. 3879–3890, Oct. 2009.
[60] A. Lanata, G. Valenza, C. Mancuso, and E. P. Scilingo, "Robust multiple cardiac arrhythmia detection through bispectrum analysis," *Expert Syst. Appl.*, vol. 38, no. 6, pp. 6798–6804, 2011.
[61] A. Barnett and R. Wolff, "A time-domain test for some types of nonlinearity," *IEEE Trans. Signal Process.*, vol. 53, no. 1, pp. 26–33, Jan. 2005.
[62] R. Kohavi and F. Provost, "Glossary of terms," *Mach. Learn.*, vol. 30, no. Jun., pp. 271–274, 1998.
[63] R. Kohavi, "A study of cross-validation and bootstrap for accuracy estimation and model selection," in *Proc. Int. Joint Conf. Artif. Intell.*, vol. 14, no. 2, pp. 1137–1145, 1995.
[64] W. KinneBrock, *Neural Networks*. Munich, Germany: Oldenburg Verlag, 1992.
[65] A. P. Association, A. P. A. T. F. on DSM-IV., *Diagnostic and statistical manual of mental disorders: DSM-IV*. Arlington, VA, USA: Amer. Psychiatric Pub. Inc., 1994.
[66] P. Lang, M. Bradley, and B. Cuthbert, *International affective picture system (IAPS): Technical manual and affective ratings*, NIMH Center for the Study of Emotion and Attention, Univ. Florida, Gainesville, FL, USA, 1999.
[67] A. Conklin and D. Westen, "Thematic apperception test," in *Understanding Psychological Assessment*. New York, NY, USA: Springer, 2001, pp. 107–133.
[68] J. P. Burg, "A new analysis technique for time series data," presented at the NATO Adv. Study Inst. Signal Process., Enschede, Netherlands, 1968, vol. 32.
[69] J. S. Chang, C. S. Yoo, S. H. Yi, J. Y. Her, H. M. Choi, T. H. Ha, T. Park, and K. Ha, "An integrative assessment of the psychophysiologic alterations in young women with recurrent major depressive disorder," *Psychosomatic Med.*, vol. 74, no. 5, pp. 495–500, 2012.
[70] J. Gruber, A. G. Harvey, and A. Purcell, "What goes up can come down? a preliminary investigation of emotion reactivity and emotion recovery in bipolar disorder," *J. Affective Disorders*, vol. 133, no. 3, pp. 457–466, 2011.
[71] B. Levy, "Autonomic nervous system arousal and cognitive functioning in bipolar disorder," *Bipolar Disorders*, vol. 15, no. 1, pp. 70–79, 2013.
[72] M. Di Simplicio, G. Costoloni, D. Western, B. Hanson, P. Taggart, and C. Harmer, "Decreased heart rate variability during emotion regulation in subjects at risk for psychopathology," *Psychol. Med.*, vol. 42, no. 8, pp. 1775–1783, 2012.
[73] C. Vögele, S. Sorg, M. Studtmann, and H. Weber, "Cardiac autonomic regulation and anger coping in adolescents," *Biol. Psychol.*, vol. 85, no. 3, pp. 465–471, 2010.
[74] J. Martin and E. Martin-Sanchez, "Systematic review and meta-analysis of vagus nerve stimulation in the treatment of depression: variable results based on study designs," *Eur. Psychiatry*, vol. 27, no. 3, pp. 147–155, 2012.
[75] C. Chang, C. D. Metzger, G. H. Glover, J. H. Duyn, H.-J. Heinze, and M. Walter, "Association between heart rate variability and fluctuations in resting-state functional connectivity," *Neuroimage*, vol. 68, pp. 93–104, 2013.
[76] J. F. Thayer, F. Åhs, M. Fredrikson, J. J. Sollers III, and T. D. Wager, "A meta-analysis of heart rate variability and neuroimaging studies: Implications for heart rate variability as a marker of stress and health," *Neurosci. Biobehavioral Rev.*, vol. 36, no. 2, pp. 747–756, 2012.
[77] A. R. Brunoni, M. Lopes, and F. Fregni, "A systematic review and meta-analysis of clinical studies on major depression and bdnf levels: Implications for the role of neuroplasticity in depression," *Int. J. Neuropsychopharmacol.*, vol. 11, no. 8, pp. 1169–1180, 2008.
[78] G. Valenza and E. P. Scilingo, "Autonomic nervous system dynamics for mood emotional-state recognition," in *Significant Advances in Data Acquisition, Signal Processing and Classification*. New York, NY, USA: Springer, 2013.

Authors' photographs and biographies not available at the time of publication.